

Estimation of Characteristic Impedance using Multi-Gaussian Modelled Flow Velocity Waveform: A Virtual Subjects Study

Rahul Manoj, Raj Kiran V, Nabeel P M, *Member IEEE*, Mohanasankar Sivaprakasam and Jayaraj Joseph

Abstract— Characteristic impedance (Z_C) of the blood vessel relates the pulsatile pressure to pulsatile blood flow velocity devoid of any wave reflections. Estimation of Z_C is useful for indirect evaluation of local pulse wave velocity and crucial for solving wave separation analysis (WSA) which separates the forward-backward pressure and flow velocity waveforms. As opposed to conventional WSA, which requires simultaneous measurement of pressure and flow velocity waveform, simplified WSA relies on modelled flow velocity waveforms, mainly introduced for the aorta. This work uses a multi-Gaussian decomposition (MGD) modelled flow velocity waveform to estimate Z_C by employing a frequency domain analysis, which is applicable to other arteries such as carotid. Thus obtained Z_C is compared with Z_C estimated from true flow velocity waveform for healthy (virtual) subjects taken for the carotid artery. The MGD modelled flow velocity waveform estimated Z_C for a range of 4.98 to 34.79 with a group average of 16.43 ± 0.10 . The difference between the group average values of both Z_C was only 4.72%. A statistically significant and strong correlation ($r = 0.708$, $p < 0.0001$) was observed for Z_C obtained from MGD modelled flow velocity waveform with Z_C obtained from actual flow velocity waveform. The bias for Z_C between the two methods was 0.74, with confidence intervals (CIs) between 7.44 and -5.96 for the Bland-Altman analysis. Therefore, Z_C from MGD modelled flow velocity waveform is a potential surrogate of the flow velocity model for WSA at the carotid artery.

Clinical Relevance— This study provides a new method to derive characteristic impedance without the measurement of actual flow velocity waveform. The method requires a single pulse waveform (pressure or diameter).

I. INTRODUCTION

Vascular impedance characterizes the arterial system by quantifying the level of energy stored and dissipated during the pulsatile flow of blood [1]. Input Impedance (Z_0) is a type of vascular impedance that can be directly measured from experimental data of pulsatile pressure and pulsatile blood flow velocity (typically at the entrance of a large artery) and is a complex number with magnitude and phase components. However, characteristic impedance (Z_C) is a type of vascular impedance that relates the pulsatile pressure and blood flow

devoid of any wave reflections. As reflections carry information of distal vasculature, Z_C makes an important local vessel parameter. Z_C varies directly with the elastic modulus of the blood vessel and inversely with diameter [2]. The behaviour of pulse wave velocity (PWV) and arterial stiffness are assessed using Z_C , and the same has been used to quantify the effects of different interventions, drugs, and diseases on pulsatile hemodynamics. The application of Z_C is not limited to its own physiological significance. Estimation of Z_C allows evaluation of local and/or incremental PWV [3], [4], calibration-free models of central BP [5], vascular ageing-related changes in reflection quantification indices (using wave separation analysis (WSA), yielding forward-backward pressure and flow velocity waveforms).

The estimation of Z_C is performed in both frequency and time domains [2]. In the frequency domain approach, Z_C is typically estimated by averaging the magnitude of Z_0 over a frequency band where one might expect fluctuations due to wave reflection above the magnitude of Z_C to cancel out oscillations below it [1]. Another method of estimating Z_C is to the average magnitude of Z_0 at high-frequency values where fluctuations caused by reflections have settled [6] (typically, an average of 4 to 10 harmonics are used). The time-domain approach to estimate Z_C involves measuring the initial upstroke of the pressure and flow velocity waveforms, as they are generally assumed reflection-free.

Conventionally, WSA involves simultaneous measurement of pressure and flow velocity waveform (ideally from the same target artery) and using either frequency or time-domain approach, Z_C is estimated. The simultaneous measurement of pressure and flow velocity waveform is an instrumentation challenge [7]. Hence, simplified WSA that uses a modelled flow velocity waveform for the estimation of Z_C and WSA was introduced [8], [9]. By incorporating flow velocity models, only pressure or diameter signals need to be measured for WSA [10]. However, such methods were developed for and validated on aortic waveforms.

In this work, we are estimating Z_C using a flow velocity model obtained from a multi-Gaussian decomposed (MGD) pressure waveform. The estimated Z_C (Z_{C-MGD}) is compared with the Z_C derived from the true flow velocity waveform (Z_{C-True}) using the frequency domain approach. The following sections describe the theory of MGD modelled flow velocity waveform, estimation of Z_C , allied results and future works.

II. MATERIALS AND METHODS

A. Theory – MGD Modelled Flow Velocity Waveform

The pressure waveform ($P(t)$) is decomposed into N Gaussian functions with their respective amplitudes (A_i , $i = 1$

Rahul Manoj and Raj Kiran V are with the Electrical Engineering Department, Indian Institute of Technology Madras, Chennai-600036, India (e-mail: rahulmanojktym@gmail.com).

Nabeel P M is with Healthcare Technology Innovation Centre (HTIC), Indian Institute of Technology Madras Research Park, Chennai-600113, India.

Jayaraj Joseph is with the faculty of Electrical Engineering Department. Mohanasankar Sivaprakasam is the Director of Healthcare Technology Innovation Centre and with the faculty of Electrical Engineering Department at Indian Institute of Technology Madras, Chennai-600036, India

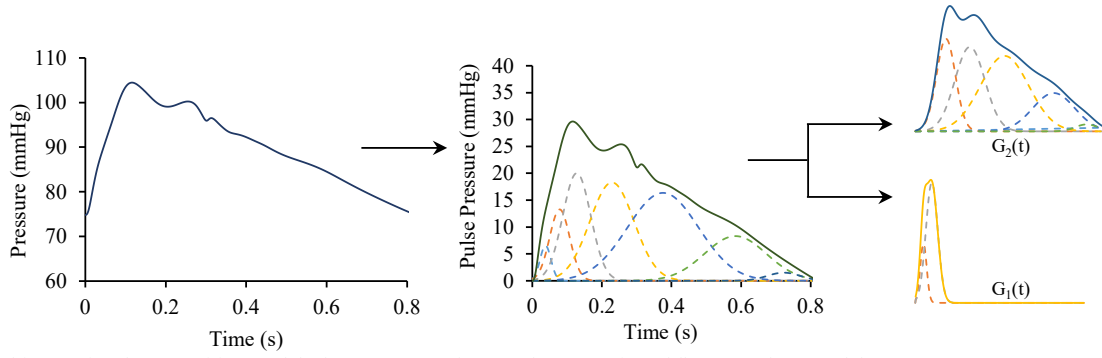


Fig.1. Multi-Gaussian decomposition model of pressure waveform, and construction of flow waveform model

to N), mean locations (M_i , $i = 1$ to N) and standard deviation locations from respective means (C_i , $i = 1$ to N), as in (1).

$$\hat{P}(t) = \sum_{i=1}^N A_i e^{-\frac{1}{2} \times \frac{(t-M_i)^2}{C_i^2}} \quad (1)$$

where $\hat{P}(t)$ is the modelled pressure waveform, $K: \{A_i, M_i, C_i\}$ is the parameter set to be optimized for curve fitting. A Levenberg-Marquardt (LM) algorithm based on the sum of weighted least squares was applied for non-linear curve fit. The individual Gaussian functions are sorted in the ascending order of their mean locations and are then uniquely combined to obtain $G_1(t)$ and $G_2(t)$. Out of the ' N ' Gaussians that decompose the pressure waveform, $G_1(t)$ is obtained from the first ' n ' among the Gaussians that exist till the dicrotic notch of $P(t)$. Further, $G_2(t)$ is obtained from the remaining ' $N - n$ ' Gaussians.

$$G_1(t) = \sum_{i=1}^n g_i(t) \quad (2)$$

$$\text{and } G_2(t) = \sum_{i=n+1}^N g_i(t) \quad (3)$$

The inflection point as obtained from higher derivative waveforms of $P(t)$ is used to classify $P(t)$ into Type-A, Type-B and Type-C [11], and a lookup table for (N, n) is generated that provides the optimal solutions for (N, n) for each type of waveform morphology from previous studies [10], [12].

Thus obtained $G_1(t)$, is the MGD modelled flow velocity waveform; proceeding further with $G_1(t)$ and $G_2(t)$, one can arrive at the wave separation analysis for separating the forward and backward waves from $P(t)$ [10], [12].

B. Data Preparation and Processing

The study population comprises of healthy (virtual) subject's database, developed by the Hemodynamic research group, Kings College, London, UK. The database is created based on 1D numerical modelling of the arterial tree. A parametric input set based on the variability of cardiac, arterial, vascular bed and blood properties for an age group of 25 – 75 years was used to create the database [13]. Pressure (in mmHg) and flow velocity waveform (in m/s) for a subset of the database for the common carotid artery is used in this study. Both the waveforms were sampled at 500 Hz. A cycle-trimming algorithm (based on end-diastole point) was

implemented to ensure uniformity across all the subjects. A linear baseline estimator compensated baseline wandering. The required higher derivatives of pressure waveform were obtained, and the subjects were classified into Type-A, Type-B and Type-C.

For estimating Z_C and to compare statistically, both the MGD modelled flow velocity waveform ($G_1(t)$) and the true flow velocity waveform ($U(t)$) obtained directly from the database were normalized from 0 to 1 with arbitrary units (AU) as illustrated in Fig.1. Frequency-domain analysis is used in this study to determine the Z_C . In this approach, the $P(t)$ and respective flow velocity waveform ($G_1(t)$ and $U(t)$) are decomposed into Fourier series components. The magnitude of input impedance (Z_0) is computed as the ratio of $P_N(t)/G_{1N}(t)$ and $P_N(t)/U_N(t)$, where $P_N(t)$, $G_{1N}(t)$ and $U_N(t)$ are N^{th} harmonics of $P(t)$, $G_1(t)$ and $U(t)$ waveforms respectively in the frequency domain. As per the theory underlined in distributed electrical networks, Z_0 is a complex quantity with magnitude and phase, whereas Z_C is a real quantity that is not entirely measurable. Z_C is the ratio of pressure and flow velocity in the frequency domain in a blood vessel devoid of any wave reflections. Since its reflection-free, the pressure and flow velocity will have the same wave shape, making Z_C a real quantity. In most cases, Z_C becomes an approximated condition of the Z_0 . Out of the decomposed components, four to ten harmonics of both $P(t)$ and respective flow velocity waveform are used to estimate the Z_C . All the algorithms were implemented in LabVIEW[®] (National Instruments, USA).

C. Statistical Analysis

All continuous variables are presented as mean \pm standard deviations. Regression analysis was performed between Z_{C-MGD} and Z_{C-True} . The correlation was reported in terms of Pearson's correlation coefficient (r) and statistical significance in the p -value. Box-and-whisker plots were used to indicate the similarity or difference between the ranges of Z_C across the population and among different waveform Types (Type-A, B, C). The level of significance of $\alpha = 0.05$ was used for all tests. A p -value > 0.05 confirmed a statistical significance.

III. RESULTS AND DISCUSSIONS

A. Reliability of MGD Modelled Flow Velocity Waveform

A comparison of the MGD-modelled flow velocity waveform ($G_1(t)$) with that of the actual flow velocity is depicted in Fig.2(a). The peaks of $G_1(t)$ and actual flow velocity were coinciding with an insignificant difference in their temporal sites (0.07 ± 0.02 s versus 0.06 ± 0.01 s; $p <$

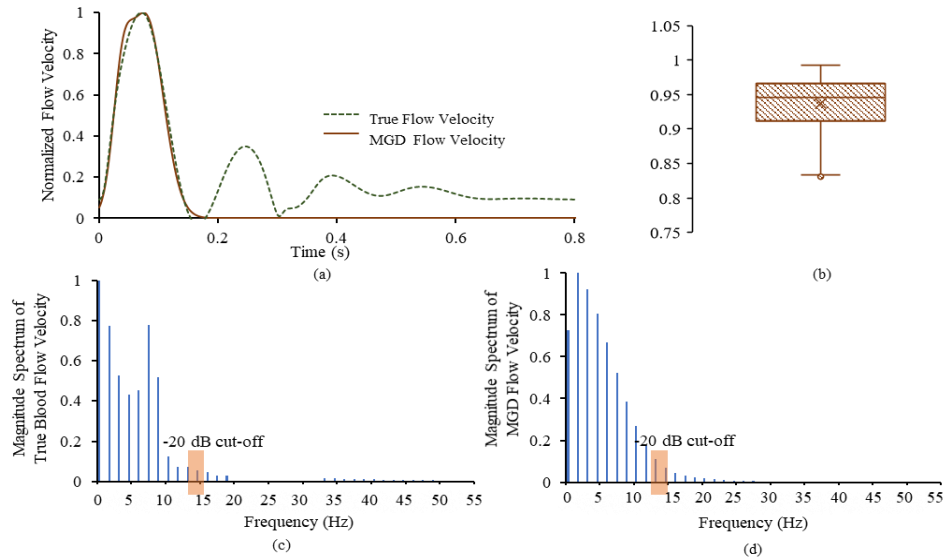


Fig.2(a). Comparison of Normalized MGD flow velocity waveform and normalized true flow velocity waveform of a sample subject, (b) range of correlation coefficient (r -value) of the amplitudes of FFT of true flow velocity and MGD modelled flow velocity, (c) FFT of true flow velocity waveform for a sample subject, (d) FFT of MGD modelled flow velocity waveform for a sample subject

0.0001, respectively). Samples of the FFT for actual flow velocity and $G_1(t)$ are depicted in Fig.2(c) and (d). The magnitude spectrum of $G_1(t)$ yielded a -20 dB cut-off within 12 – 14 Hz, which was also exhibited by the magnitude spectrum of the actual flow velocity. The amplitudes of their magnitude spectrum found to correlate significantly high ($p < 0.001$) with a group average correlation coefficient $r = 0.93 \pm 0.03$, ranged between 0.83 – 0.99 (Fig.2(b)). Consistent with the theory [14], about 95 – 97 percentile of the flow velocity frequency content was within the first 15 harmonics in the frequency domain. Previous studies [20] reported that the systolic phase of the flow waveform has more influence on the estimation of the Z_C , and the FFT results supplement it.

B. Estimation of Characteristic Impedance

The MGD modelled flow velocity waveform was able to estimate Z_C for a range of 4.98 to 34.79 with a group average of 16.43 ± 0.10 . The Z_C from true flow velocity waveform was for a range of 5.80 to 31.37, with a group average of 15.69 ± 0.10 . The difference between the group average values of both Z_C was only 4.72%. Fig.3(c) highlights the range of Z_C for the entire population, and Fig.3(d) shows the deviations of Z_C for each Type of waveform morphology across the study population.

A statistically significant and strong correlation ($r = 0.708$, $p < 0.0001$) was observed for Z_C obtained from MGD modelled flow waveform with Z_C obtained from actual flow waveform as depicted in Fig.3(a). Bland-Altman plot, as depicted in Fig. 3(b), reveals a scattered graph with no clear trend of systemic progression of errors. The bias for Z_C between the two methods was 0.74 AU (4.5% of the group average Z_{C-MGD}) with confidence intervals (CIs) between 7.44 AU (45% of the group average Z_{C-MGD}) and -5.96 AU (36% of the group average Z_{C-MGD}). Similar ranges were reported in the literature for bias and CIs (bias is 8% of the respective model Z_C and CIs are 45% and 35% of the respective model Z_C) [15].

Accuracy in the estimation of Z_C is determined by the accuracy of the modelled flow velocity waveform. Although

Z_C is a cardiovascular marker by itself, the importance of accurately determining Z_C expands to estimating reflection markers such as reflection magnitude, reflection index and reflection wave transit time accurately. All reflection markers are obtained using WSA either in the frequency domain or time domain. Either way, part of the solution of WSA involves the determination of Z_C , and Z_{C-MGD} was found to be strongly correlated with the Z_{C-true} for the carotid artery and therefore is a potential surrogate of flow velocity model for WSA. Likewise, similar flow velocity modelling approaches [8], [9], [16] simplify the conventional WSA to a single pulse technique (depending only on pressure waveform); Such techniques, reported previously in the literature, were found only to be applied for aortic flow velocity modelling and have a significant correlation with the Z_{C-True} of the aorta [15]. However, further studies are needed to explore if the aforesaid models can be applied to non-aortic sites such as the carotid artery.

As the future scope for large scale field studies, the applicability of Z_C derived from diameter waveforms [17], [18] has potential for large scale screening using non-invasive instrumentations [19], [20] needs to be explored for a better understanding of central haemodynamics. The advent of wearable platforms enables continuous monitoring of ECG [21], [22], heart rate [23], respiratory rate [24], [25], when combined with Z_C assessment, would provide further insights into the dynamics of central arteries.

IV. CONCLUSION

This work has demonstrated the accuracy of Z_C obtained using multi-Gaussian decomposed flow velocity waveform constructed from the pressure waveform. Z_{C-MGD} was compared with the Z_{C-True} that is obtained from the true flow velocity waveform. Both Z_C found a statistically significant and strong correlation with negligible bias. The potential application of the method involves the wave separation analysis using modelled flow waveform for the carotid artery.

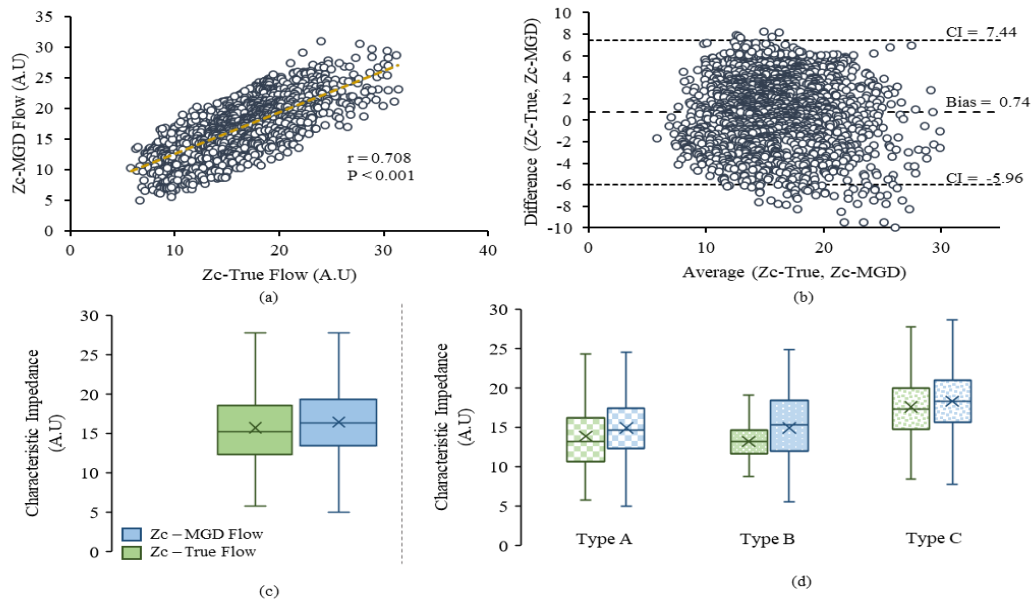


Fig.3. (a)-(b) Correlation plot waveform and Bland-Altman Analysis for Z_c obtained from MGD modelled flow velocity waveform and true flow velocity, (c)-(d) Range of Z_c obtained from across the population and for each type of the pressure waveform morphology

The method was validated across different types of wave morphologies across a broad age group.

REFERENCES

- [1] W. W. Nichols et al., *McDonald's blood flow in arteries theoretical, experimental and clinical principles*. 2011.
- [2] M. U. Qureshi et al., "Characteristic impedance: Frequency or time domain approach?," *Physiol. Meas.*, vol. 39, no. 1, 2018.
- [3] P. M. Nabeel et al., "A Magnetic Plethysmograph Probe for Local Pulse Wave Velocity Measurement," *IEEE Trans. Biomed. Circuits Syst.*, vol. 11, no. 5, pp. 1065–1076, 2017.
- [4] P. M. Nabeel et al., "Variation in local pulse wave velocity over the cardiac cycle: in-vivo validation using dual-MPG arterial compliance probe," *13th Russ. Conf. Biomed. Eng.*, pp. 100–103, 2018.
- [5] P. M. Nabeel et al., "Bi-Modal arterial compliance probe for calibration-free cuffless blood pressure estimation," *IEEE Trans. Biomed. Eng.*, vol. 65, no. 11, pp. 2392–2404, 2018.
- [6] N. Westerhof, et al., "Forward and backward waves in the arterial system," *Cardiovasc. Res.*, vol. 6, no. 6, pp. 648–656, 1972.
- [7] A. P. G. Hoeks, J. M. Willigers, and R. S. Reneman, "Effects of assessment and processing techniques on the shape of arterial pressure-distension loops," *J. Vasc. Res.*, vol. 37, no. 6, pp. 494–500, 2000.
- [8] B. E. Westerhof et al., "Quantification of wave reflection in the human aorta from pressure alone: A proof of principle," *Hypertension*, vol. 48, no. 4, pp. 595–601, 2006.
- [9] B. Hametner et al., "Wave reflection quantification based on pressure waveforms alone-methods, comparison, and clinical covariates," *Comput. Methods Programs Biomed.*, vol. 109, no. 3, pp. 250–259, 2013.
- [10] R. Manoj et al., "Separation of Forward-Backward Waves in the Arterial System using Multi-Gaussian Approach from Single Pulse Waveform," in *Proceedings of the Annual International Conference of the IEEE Engineering in Medicine and Biology Society, EMBS*, 2021, vol. 2021, pp. 5547–5550.
- [11] J. P. Murgo et al., "Impedance in," *Circ. J.*, vol. 62, no. 1, pp. 105–116, 1980.
- [12] R. Manoj et al., "Evaluation of Nonlinear Wave Separation Method to Assess Reflection Transit Time: A Virtual Patient Study," in *Proceedings of the Annual International Conference of the IEEE Engineering in Medicine and Biology Society, EMBS*, 2021, vol. 2021, pp. 5551–5554.
- [13] P. H. Charlton et al., "Modeling arterial pulse waves in healthy aging: a database for in silico evaluation of hemodynamics and pulse wave indexes," *Am. J. Physiol. - Hear. Circ. Physiol.*, vol. 317, no. 5, pp. H1062–H1085, 2019.
- [14] D. W. Holdsworth et al., "Characterization of common carotid artery blood-flow waveforms in normal human subjects," *Physiol. Meas.*, vol. 20, no. 3, pp. 219–240, 1999.
- [15] B. Hametner et al., *Effects of Different Blood Flow Models on the Determination of Arterial Characteristic Impedance*, vol. 45, no. 2. IFAC, 2012.
- [16] J. G. Kips et al., "Evaluation of non-invasive methods to assess wave reflection and pulse transit time from the pressure waveform alone," *Hypertension*, vol. 53, no. 2, pp. 142–149, 2009.
- [17] A. K. Sahani et al., "Automatic measurement of end-diastolic arterial lumen diameter in ARTSENS," *J. Med. Devices, Trans. ASME*, vol. 9, no. 4, Aug. 2015.
- [18] A. K. Sahani et al., "Automated system for imageless evaluation of arterial compliance," *Proc. Annu. Int. Conf. IEEE Eng. Med. Biol. Soc. EMBS*, pp. 227–231, 2012.
- [19] J. Joseph et al., "Assessment of Carotid Arterial Stiffness in Community Settings with ARTSENS®," *IEEE J. Transl. Eng. Heal. Med.*, vol. 9, no. November 2020, 2021.
- [20] J. Joseph et al., "ARTSENS® Pen - Portable easy-to-use device for carotid stiffness measurement: Technology validation and clinical-utility assessment," *Biomed. Phys. Eng. Express*, vol. 7, no. 2, 2020.
- [21] S. P. Preejith et al., "Wearable ECG platform for continuous cardiac monitoring," *Annu. Int. Conf. IEEE Eng. Med. Biol. Soc. IEEE Eng. Med. Biol. Soc. Annu. Int. Conf.*, vol. 2016, pp. 623–626, Oct. 2016.
- [22] B. Murugesan et al., "ECGNet: Deep Network for Arrhythmia Classification," in *MeMeA 2018 - 2018 IEEE International Symposium on Medical Measurements and Applications, Proceedings*, 2018.
- [23] S. P. Preejith et al., "Design, development and clinical validation of a wrist-based optical heart rate monitor," *2016 IEEE Int. Symp. Med. Meas. Appl. MeMeA 2016 - Proc.*, Aug. 2016.
- [24] V. Ravichandran et al., "RespNet: A deep learning model for extraction of respiration from photoplethysmogram," in *Proceedings of the Annual International Conference of the IEEE Engineering in Medicine and Biology Society, EMBS*, 2019, pp. 5556–5559.
- [25] S. P. Preejith, A. Jeelani, P. Maniyar, J. Joseph, and M. Sivaprakasam, "Accelerometer based system for continuous respiratory rate monitoring," *2017 IEEE Int. Symp. Med. Meas. Appl. MeMeA 2017 - Proc.*, pp. 171–176, Jul. 2017.